

Electronic Supplementary Information

Exfoliation of Bimetallic (Ni, Co) Carbonate Hydroxide Nanowires by Ar Plasma for enhanced oxygen evolution

Hongmei Sun,^a Yuanling Miao,^a Tao Wu,^b and Qi Wang^{*a, b}

^a Key Laboratory of Photovoltaic and Energy Conversation Materials, Institute of Plasma Physics, Hefei Institutes of Physical Science, Chinese Academy of Sciences, Hefei 230031, China.

^b College of Chemistry, Chemical Engineering and Materials Science, Soochow University, Suzhou, Jiangsu 215123, China

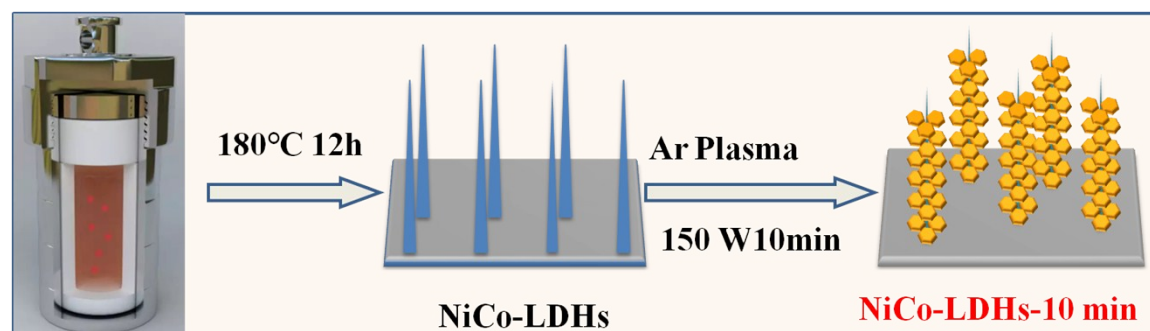
S1. Experimental section

Chemical Reagents and Materials

All chemicals in this experiment were analytical grade and applied without further purification. Cobalt chloride hexahydrate, nickel chloride hexahydrate, polyvinyl pyrrolidone and urea were purchased from Aladdin Industrial Corporation (Shanghai, China).

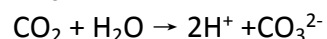
Synthesis of 1 D NiCo-LDHs nanowires

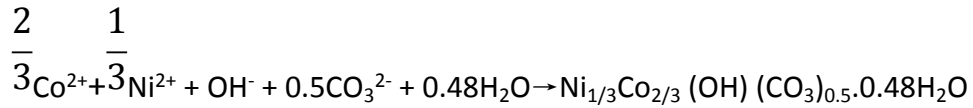
In a typical experiment, 15.0 mg polyvinyl pyrrolidone (PVP, Mw $\frac{1}{4}$ 130 000, K90-96) was dissolved in 15.0 ml deionized water under magnetic stirring at room temperature. Then, 0.474 g cobalt chloride hexahydrate, 0.237 g nickel chloride hexahydrate and 0.60 g of urea were added to the solution mixture under magnetic stirring. The resultant mixture was stirred continually for 15 min until a homogeneous pink solution was obtained, which was then transferred into a Teflon-lined stainless steel autoclave (capacity of 50 ml). The autoclave was sealed and maintained at 180 °C for 12 h in an oven. The precursor product was then collected and washed with distilled water as well as absolute alcohol several times, followed by vacuum-drying at 80 °C for 6 h. The obtained sample was denoted as NiCo-LDHs.



Scheme S1 shows the preparation process of the composites

The reactions involved in the system could be described as following:¹





Exfoliation of NiCo-LDHs nanowires by Ar plasma

The obtained NiCo-LDHs nanowires were treated by radio frequency inductively coupled plasma (RF-ICP) with RF frequency of 13.56 MHz, the power 200 W, the Ar flow rate of 15 sccm, the pressure of 15 Pa and the treatment time of 10 min, which was denoted as NiCo-LDHs-10min. For compared, when the treatment time was 0 min, 5 min, 15 min and 30 min, the obtained sample was denoted as NiCo-LDHs-0min, NiCo-LDHs-5min, NiCo-LDHs-15min and NiCo-LDHs-30min, respectively.

Materials Characterization

The morphologies and microstructures of the samples were observed by transmission electron microscopy (TEM, GF-20). The powder X-ray diffraction (XRD) patterns were determined by using a Cu-K α radiated ($\lambda = 1.5419 \text{ \AA}$) Philips X'Pert system. The surface elemental compositions and chemical state analysis were determined using X-ray photoelectron spectroscopy (XPS; Thermo ESCALB 250). Nitrogen adsorption-desorption isotherms were measured on a Ommishop 100CX at 473 K. The specific surface areas were calculated by the Brunauer-Emmet-Teller (BET) methods. Thermogravimetric analysis of the samples was performed by using a DSC204F1 thermal analysis instrument in argon, and the heating rate was $10^\circ\text{C min}^{-1}$. Fourier transform infrared spectra were obtained with NEXUS (Thermo Nicolet Corporation, America) at a resolution of 2 cm^{-1} and averaging ten scans in the $400\text{-}4000 \text{ cm}^{-1}$ region on pressed KBr pellets. The Raman spectra (RS) was conducted at 532 nm with a laser power of $\sim 1 \text{ mW}$ using a DXR Microscope Raman spectrometer system.

S2 Electrochemical measurement of NiCo-LDHs

The OER tests were performed with an electrochemical workstation (CHI 660D, ChenHua Instrument, China). Pt foil and Hg/HgO were used as the counter and reference electrodes, respectively. 1 M KOH solution was used as the electrolyte. Note that the current density was standardized to a geometrical surface area and all potentials vs. Hg/HgO were converted to a reversible hydrogen electrode (RHE) scale according to the following Nernst equation ($E_{\text{RHE}} = E_{\text{Hg/HgO}} + 0.059\text{pH} + 0.098V = E_{\text{Hg/HgO}} + 0.924\text{V}$), where $E_{\text{Hg/HgO}}$ is the experimentally measured potential against the Hg/HgO (1 M NaOH) reference electrode. The overpotential (η) was calculated according to the following formula: $\eta \text{ (V)} = E_{\text{RHE}} - 1.23 \text{ V}$. Tafel slopes were calculated based on the following equation: $\eta = a + b \log j$, where η is the overpotential, j is the current density, and b is the Tafel slope. The linear sweep voltammetry (LSV) tests were conducted at a scan rate of 5 mV/s , which were measured after 10 cycles of LSV test in the range of 0.2 to 0.6 V vs Hg/HgO to stabilize the current at 50 mV/s . The Tafel plots were derived from LSV. The ohmic potential drop (iR) arising from the resistance of the electrolyte solution was compensated at a rate 80% by default through CHI-660e software. Then the ECSA was determined by measuring the capacitive current associated with double-layer charging from the scan-rate dependence of CVs. For this, the potential window of CV was $0.1\text{-}0.2 \text{ V}$ vs Hg/HgO. The scan rates were 5, 10, 15, 20, 25 and 30 mV/s . The

double layer capacitance (C_{dl}) was estimated by plotting the $\Delta J = (J_a - J_c)$ at 1.08 V vs. RHE against the scan rate. The linear slope is twice of the double layer capacitance C_{dl} .² The electrochemical impedance spectroscopies (EIS) of NiCo-LDHs-10min and NiCo-LDHs-0min were carried out at 1.48 V and 1.6 V, where the current density of the prepared catalyst was 10 mA cm^{-2} , in a frequency from range 100 kHz to 0.01 Hz with an AC amplitude of 5 mV.

Results

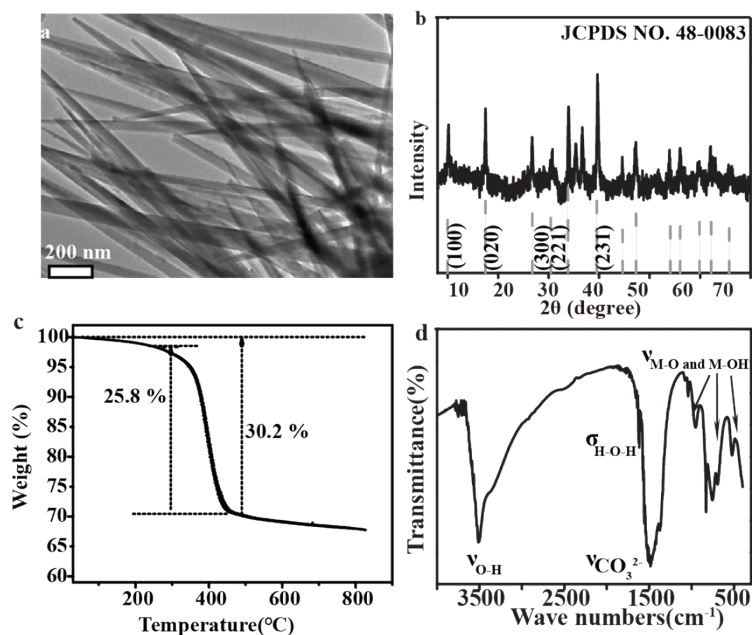


Figure S1 (a) The TEM, (b) X-ray diffraction (XRD) patterns, (c) TG analysis and (d) the Fourier-transformed infrared (FTIR) spectra of NiCo-LDHs-0min.

The TEM and X-ray diffraction (XRD) patterns of NiCo-LDHs-0min are shown in Figure S1a, b. The NiCo-LDHs-0min exists as smooth needle-like nanorods (Figure S1a). The diffraction peaks of NiCo-LDHs-0min (Figure S1b) at 17.29° , 33.74° and 35.48° are the overlap of (020), (221) and (040) planes of the $\text{Co}(\text{CO}_3)_{0.5}(\text{OH}) \cdot 0.11\text{H}_2\text{O}$ (JCPDS card, no. 48-0083) and (120), (-121), and (240) planes of $\text{Ni}_2(\text{CO}_3)(\text{OH})_2$ (JCPDS card, no. 35-0501).^{1,2} The thermogravimetry (TG) analysis (Figure S1c) of NiCo-LDHs-0min exhibits two successive decomposing stages, corresponding to the dehydration and decarboxylation/dehydration processes, respectively. A major thermal event takes place at 300°C - 450°C during the heating process, corresponding to a weight loss of 25.8 % for the total weight loss, originating from the decomposition of this solid precursor into NiCo_2O_4 , CO_2 and H_2O . This value is nearly the theoretical value (25.64%) for this thermal decomposition.¹ Fourier-transformed infrared (FTIR) spectra (Figure S1d) also confirms the formation of a hydroxylated structure. The characteristic bands of brucite-like metal hydroxide layers are observed: 3471 and 1619 cm^{-1} arise from O-H stretching vibration and the H-O-H bending vibration of H_2O , respectively, suggesting the existence of crystal water in the as-synthesized products.³ The narrow bands at 1480 , 834 and 757 cm^{-1} are ascribed to the stretching vibration,

in-plane and out-of-plane bending vibration of CO_3 .³⁻⁵ The peaks at 957, 522, 693 cm^{-1} correspond to $\delta(\text{Co-OH})$, $\rho_w(\text{Co-OH})$ and $\nu(\text{Ni-O})$ stretching vibrations bending modes.⁶ The concentration of Ni and Co in the NiCo-LDHs was investigated by inductively coupled plasma measurement (ICP) and summarized in Table 1. The Ni:Co atomic ratio of NiCo-LDHs-0min and NiCo-LDHs-10min is 1:1.94 and 1:2.16, respectively. This result is consistent with the ratio of precursor 1:2. So the formation can be expressed by $\text{Ni}_{1/3}\text{Co}_{2/3}(\text{OH})(\text{CO}_3)_{0.5}\cdot 0.48\text{H}_2\text{O}$.

Table 1 The content of Ni and Co in the NiCo-LDHs-0min and NiCo-LDHs-10min

	NiCo-LDHs-0min	NiCo-LDHs-10min
Ni (ppm)	5.53	5.61
Co (ppm)	10.36	11.69
the atomic ratio of Ni and Co	1:1.94	1:2.16

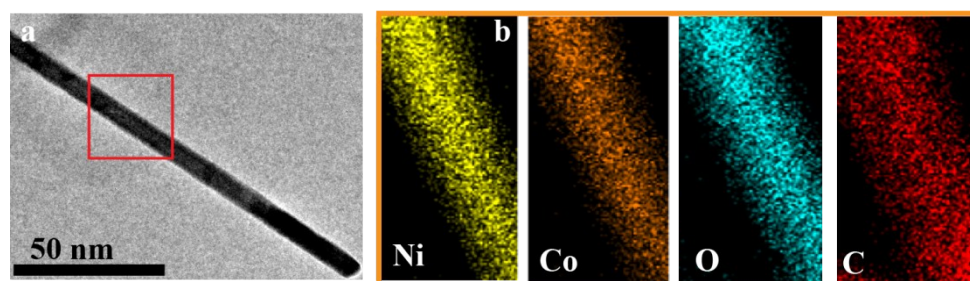


Figure S2 (a) Typical low-magnification TEM image, (b) the elemental mapping images of Ni, Co, O and C atom distributions in the area in (a).

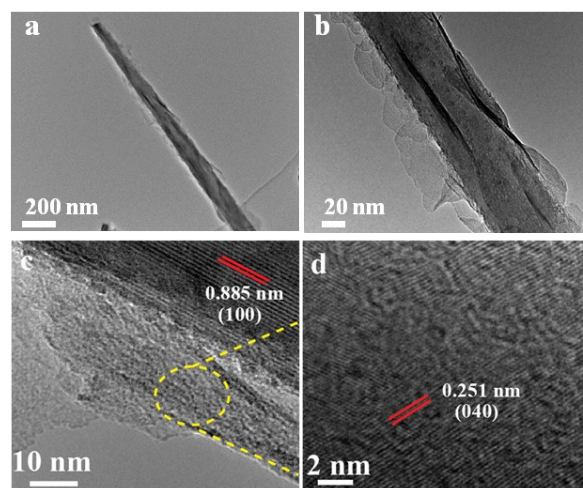


Figure S3 TEM images of NiCo-LDHs with Ar plasma treated by 30min

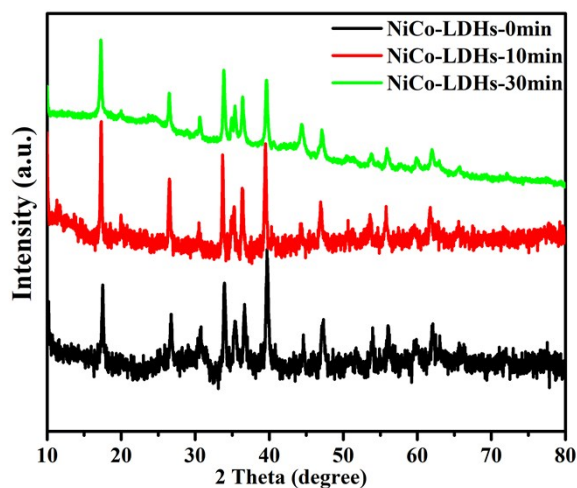


Figure S4 XRD patterns of NiCo-LDHs by the treatment of Ar plasma (0 min, 10min, 30min)

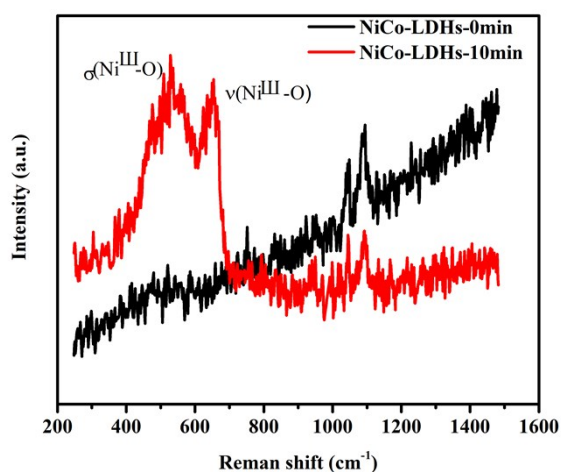


Figure S5 Raman of NiCo-LDHs-0min and NiCo-LDHs-10min

Table S2 Comparison of the catalytic activities toward the OER in 1.0 M KOH solution of the NiCo-LDHs-10min with other reported high-performance OER.

Materials	Overpotential s at 10mA cm ⁻²	Tafel slope (mV dec ⁻¹)	Reference
NiCo-LDHs-10min	250	89	This work
NiFe LDH-NS@DG10	210	52	7
CoMn LDH	324	43	8
Ni-Co nanowires/ carbon fiber	302	46	9

CoO-MoO ₂ Nanocages	312	69	10
FeCo-N-C	330	99.5	11
NiFe LDH nanosheets/ Cu nanowire	310	460	12
Dendritic Copper Oxide	290	89	13

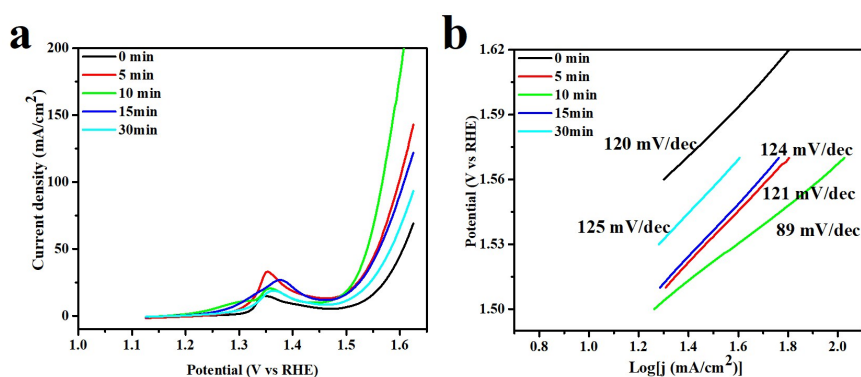


Figure S6. a) The polarization curves and (b) Tafel plots of NiCo-LDHs by the treatment of Ar plasma (0 min, 5 min, 10min, 15min, 30min).

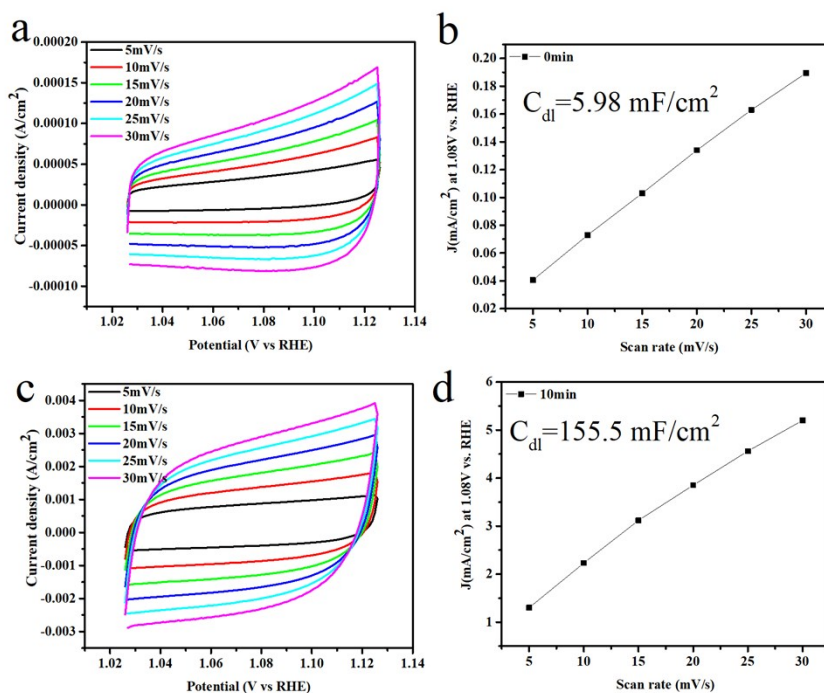


Figure S7. Cyclic voltammetry curves of a) NiCo-LDHs-0min and c) NiCo-LDHs-10min. The capacitive current measured at 1.08 V vs RHE was plotted as a function of scan rate b) NiCo-LDHs-0min and d) NiCo-LDHs-10min.

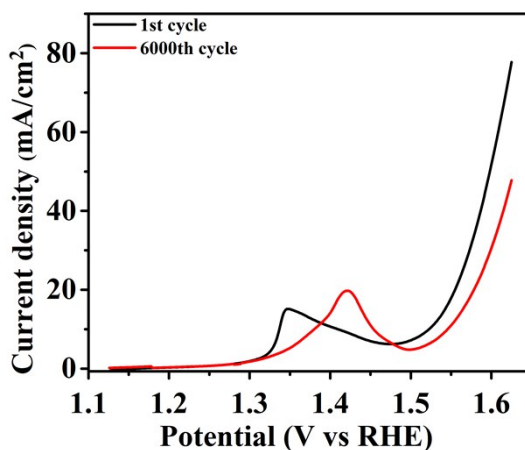


Figure S8 Stability of NiCo-LDHs-0min after 6000 cycles.

Reference

- 1 S. L. Xiong, J. S. Chen, X. W. Lou and H. C. Zeng, *Adv. Funct. Mater.*, 2012, **22**, 861.
2. H. Y. Chen, Y. R. Kang, F. Cai, S. Zeng, W. W. Li, M. H. Chen and Q. W. Li, *J. Mater. Chem. A*, 2015, **3**, 1875.
- 3 F. Song and X. Hu, *J. Am. Chem. Soc.*, 2014, **136**, 16481.
- 4.G. Zhu, C. Xi, M. Shen, C. Bao and J. Zhu, *ACS Appl. Mater. Interfaces*, 2014, **6**, 17208.
- 5 P. Vialat, C. Mousty, C. Taviot-Gueho, G. Renaudin, H. Martinez, J. C. Dupin, E. Elkaim and F. Leroux, *Adv. Funct. Mater.*, 2014, **24**, 4831.
- 6 L. P. Zhu, Z. Wen, W. M. Mei, Y. G. Li and Z. Z. Ye, *J. Phys. Chem. C*, 2013, **117**, 20465.
7. Y. Jia, L. Zhang, G. Gao, H. Chen, B. Wang, J. Zhou, M.T. Soo, M. Hong, X. Yan, G. Qian, J. Zou, A. Du and X. Yao, *Adv. Mater.* 2017, **29**, 1700017
8. F. Song and X. Hu, *J. Am. Chem. Soc.* 2014, **136**, 16481
9. S. H. Bae, J. E. Kim, H. Randriamahazaka, S. Y. Moon, J. Y. Park and I. K. Oh, *Adv. Energy Mater.* 2017, **7**, 1601492
10. F. Lyu, Y. Bai, Z. Li, W. Xu, Q. Wang, J. Mao, L. Wang, X. Zhang and Y. Yin, *Adv. Funct. Mater.* 2017, **27**, 1702324
11. C. Y. Su, H. Cheng, W. Li, Z. Q. Liu, N. Li, Z. Hou, F. Q. Bai, H. X. Zhang and T. Y. Ma, *Adv. Energy Mater.* 2017, **7**, 1602148
12. L. Yu, H. Zhou, J. Sun, F. Qin, F. Yu, J. Bao, Y. Yu, S. Chen and Z. Ren, *Energy Environ. Sci.*, 2017, **10**, 1820.
13. H. Tran Ngoc, G. Rousse, S. Zanna, I.T. Lucas, X. Xu, N. Menguy, V. Mougél, and M. Fontecave *Chem. Int. Ed.* 2017, **129**, 4870